

# Molecular Imaging of Atherosclerosis Using a Technetium-99m-Labeled Endothelin Derivative

Ludger M. Dinkelborg, Stephan H. Duda, Hartmut Hanke, Gunnar Tepe, Christoph S. Hilger and Wolfhard Semmler  
*Research Laboratories of Schering AG, Berlin; Abteilung für Radiologische Diagnostik, Eberhard-Karls Universität Tübingen, Tübingen; Medizinische Klinik, Abteilung für Kardiologie, Universität Ulm, Ulm; and Institut für Diagnostikforschung an der Freien Universität Berlin, Berlin, Germany*

Endothelins have been implicated in the pathogenesis of atherosclerosis and restenosis. The aim of this study was to characterize the potential of an endothelin derivative labeled with  $^{99m}\text{Tc}$  for imaging experimental atherosclerosis *in vivo*. **Methods:** Atherosclerosis was induced by balloon denudation of the infrarenal aorta in eight New Zealand white rabbits followed by a 6-wk period of a standard or 0.5% cholesterol diet in four animals, respectively. Another four rabbits served as controls, without balloon denudation and cholesterol feeding. Digital subtraction angiograms and planar whole-body scintigrams were obtained after intravenous injection of 74 MBq of the  $^{99m}\text{Tc}$ -labeled endothelin derivative. The aorta was dissected for autoradiography, sudan-III staining, morphometry and immunohistology (anti- $\alpha$ -actin, RAM 11) 5 hr after injection. **Results:** The lesions induced in the infrarenal aorta could be detected *in vivo* (whole-body scintigrams) in all treated animals only 15 min after injection of  $^{99m}\text{Tc}$ -endothelin derivative. Autoradiography of the excised aorta revealed good correlation of tracer accumulation and sudan-III-stained lesions. The ratio of accumulation between the induced lesions and untreated vessel wall was  $6.8 \pm 1.4$  in the cholesterol-fed animals and  $6.3 \pm 1.8$  in the animals without cholesterol feeding. Accumulation of the endothelin derivative correlated with the number of smooth muscle cells ( $r = 0.924$ ) but not with the amount of macrophages, the area or the maximum thickness of the plaques. **Conclusion:** Scintigraphic visualization of experimentally induced atherosclerosis *in vivo* is feasible using an endothelin derivative labeled with  $^{99m}\text{Tc}$ .

**Key Words:** balloon angioplasty; restenosis; neointimal formation; radiopharmaceuticals; technetium-99m-ZK 167054.

**J Nucl Med 1998; 39:1819–1822**

Today atherosclerotic lesions are diagnosed by angiography, ultrasound, CT and MRI. These diagnostic procedures are most effective in detecting advanced lesions with severe compromise of blood flow. However, they yield little information on the underlying pathophysiology such as the cellular composition of the plaque. The proliferation and migration of vascular smooth muscle cells is a crucial step during atherogenesis and in the restenosis process after balloon angioplasty (1,2). These smooth muscle cells express endothelin receptors, which are located in the sarcolemma (3,4). The aim of this study was to evaluate the diagnostic potential of a  $^{99m}\text{Tc}$ -labeled endothelin derivative for imaging atherosclerosis in a rabbit model using plaque development by endothelial denudation (5).

## MATERIALS AND METHODS

The endothelin derivative  $^{99m}\text{Tc}$ -ZK 167054 investigated is a tridecapeptide with the primary sequence of Asp-Gly-Gly-Cys-Gly-Cys-Phe-(D-Trp)-Leu-Asp-Ile-Ile-Trp. The C-terminal heptapeptide Phe-(D-Trp)-Leu-Asp-Ile-Ile-Trp of this endothelin derivative is a modified sequence of the C-terminal hexapeptide of

the endothelin family His-Leu-Asp-Ile-Ile-Trp. The C-terminal hexapeptide of the endothelin family, and derivatives thereof, have a micro- to nanomolar affinity to endothelin-A and -B receptors (6). The N-terminal hexapeptide of the endothelin derivative Asp-Gly-Gly-Cys-Gly-Cys serves as a binding core for  $^{99m}\text{Tc}$ . Labeling of the endothelin derivative with  $^{99m}\text{Tc}$  was achieved with yields higher than 95%, as determined by high pressure liquid- and thin-layer chromatography. X-ray absorption spectroscopy revealed that coordination of the  $[\text{TcO}]^{3+}$  core is restricted to the sequence -Cys-Gly-Cys-. The preferred coordination of the cysteinyl thiol group prevents involvement of any donor atom other than sulfur, thus forming purely S-coordinate 1:2 complexes (7).

## Balloon Denudation

Twelve male New Zealand white rabbits (3.0–3.5 kg body weight) were used. Animal care complied with good laboratory practice principles, and the study was approved by the Institutional Board for Laboratory Animal Care. All interventions and imaging procedures were done under general anesthesia (22 mg ketamine/kg body weight, 4.5 mg xylazine/kg body weight and 0.7  $\mu\text{g}$  atropine sulfate/kg body weight). Eight animals underwent balloon denudation of the right iliac artery and the infrarenal aorta with a 2 French Fogarty arterial embolectomy catheter (Baxter, Unterschleißheim, Germany). After intervention, four rabbits were fed a 0.5% cholesterol diet. The other four rabbits were fed a standard diet and served as a control group without undergoing balloon denudation.

## Imaging

Six weeks after plaque induction by balloon denudation, the rabbits received an injection of 5 ml iotrolan (Schering, Berlin, Germany) through the auricular vein while under general anesthesia (see above). Biplanar, transvenous, digital subtraction angiograms were obtained using a Siremobil 2000 (Siemens, Erlangen, Germany) digital subtraction angiography unit. After angiography, 74 MBq  $^{99m}\text{Tc}$ -labeled endothelin derivative were injected intravenously and planar whole-body scintigrams were obtained (acquisition time, 5 min) using an Apex SP4 HR gamma camera (Elscint, Haifa, Israel).

## Autoradiography and Sudan-III Staining

Five hours after intravenous injection of 74 MBq  $^{99m}\text{Tc}$ -endothelin derivative, the animals were killed by intravenous injection of 0.4 g embutramide, 0.1 g mebendazone iodide and 0.01 g tetracaine hydrochloride (T 61; Hoechst, Unterschleißheim, Germany). To quantitatively determine  $^{99m}\text{Tc}$ -endothelin derivative accumulation, each aorta was scanned using a PhosphorImager (Molecular Dynamics, Sunnyvale, CA) for quantitative autoradiography. Sudan-III staining of the aorta was performed subsequently for visualization of atherosclerotic lesions.

## Immunohistology

Small areas of excised vessels were immersion fixed in 2% paraformaldehyde solution and embedded in paraffin for histological preparation. Arterial segments were cut to 4  $\mu\text{m}$  thickness and

Received Oct. 2, 1997; revision accepted Jan. 14, 1998.

For correspondence or reprints contact: Ludger M. Dinkelborg, PhD, Schering AG, Forschung Molekulare Diagnostik, 13342 Berlin, Germany.

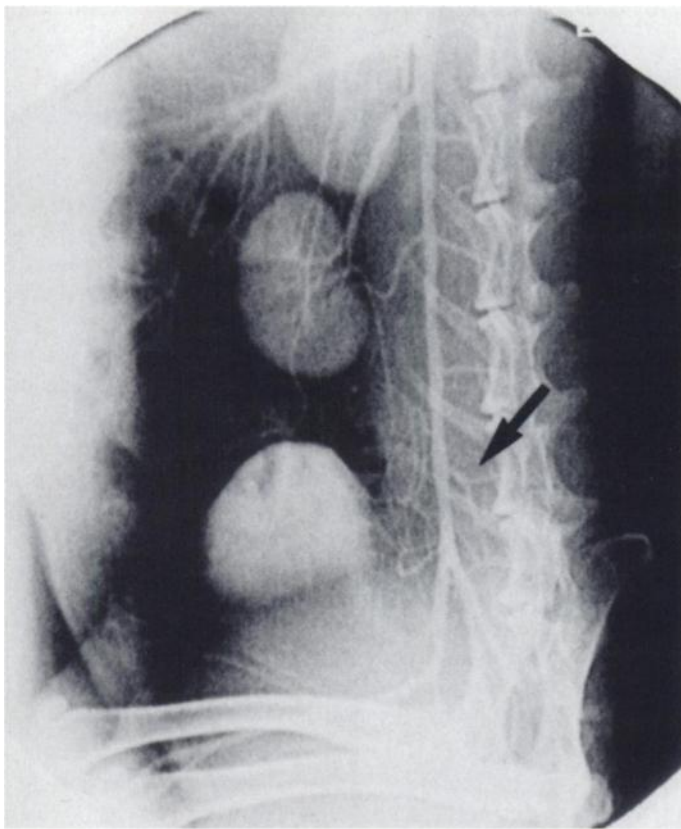


**FIGURE 1.** Left lateral angiogram of New Zealand white rabbit fed 0.5% cholesterol diet for 6 wk after balloon denudation. No stenosis was seen in infrarenal aorta (arrow).

stained with hematoxylin-eosin. The area and maximum thickness of the neointima were calculated using a digital image analyzer (Leitz, Wetzlar, Germany; software from Bilaney Consulting, Düsseldorf, Germany). Vascular smooth muscle cells and macrophages were detected and calculated using immunohistological staining with anti- $\alpha$ -actin and the RAM 11 antibody, respectively (both from Dianova, Hamburg, Germany). Statistical analysis was performed with the Student's t-test. Significance was assumed at  $p < 0.05$ . Correlation coefficients were determined using Sigma Plot (Jandel Scientific, Erkrath, Germany).

## RESULTS

Rabbits treated by balloon denudation of the infrarenal aorta ( $n = 8$ ) developed neointimal hyperplasia without recognizable narrowing of the vessel lumen. On a left lateral angiogram (Fig. 1), the infrarenal aorta, bifurcation, iliac arteries, urinary bladder, kidneys, both femora and vertebral column are depicted. The neointimal lesions induced in the infrarenal aorta of all animals were too small to be detected by x-ray angiography (Fig. 1, arrow). Left lateral scintigrams of control rabbits ( $n = 4$ ) 15 min after intravenous injection of the  $^{99m}\text{Tc}$ -endothelin derivative (Fig. 2A) showed high activity in heart, liver, kidneys, bladder, lung and abdominal aorta. The endothelin derivative underwent rapid renal elimination, because activity was already detected in the bladder at this early point in time. Four hours after injection, approximately 50% of the injected dose had been eliminated renally, and the bladder, kidney and intestine displayed high levels of radioactivity. Activity in organs like heart, liver and lung, which are known to express endothelin receptors in high amounts, was still visible. The lesions induced in the infrarenal aorta were detected in vivo in all animals treated ( $n = 8$ ) only 15 min after injection of the

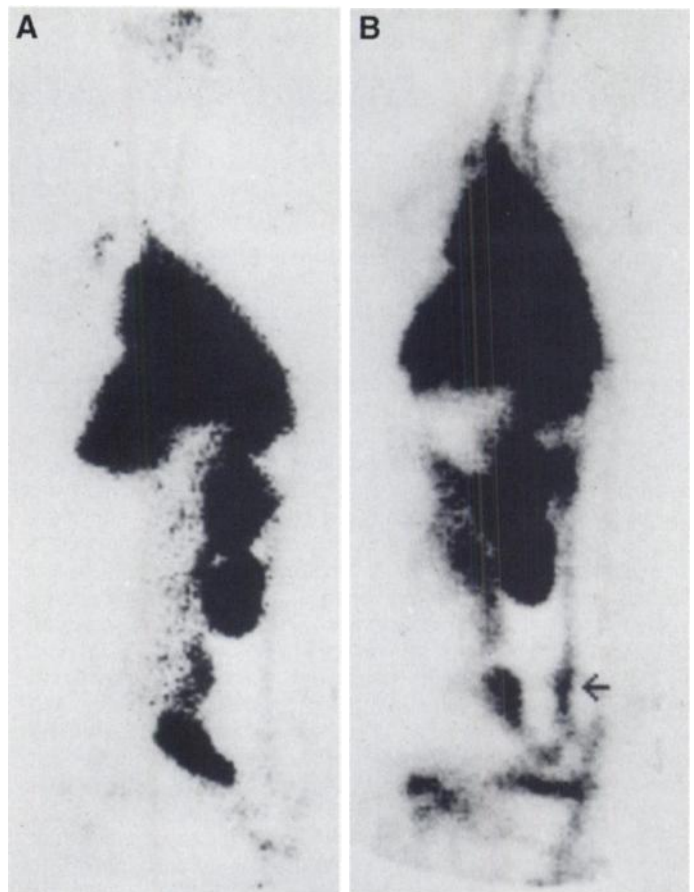


**FIGURE 2.** Left lateral scintigrams of (A) a control rabbit and (B) a rabbit after balloon denudation. Atherosclerotic lesions located in infrarenal aorta (arrow) were imaged in vivo 15 min after injection of  $^{99m}\text{Tc}$ -endothelin derivative. Further accumulation occurred in heart, liver and kidneys.

$^{99m}\text{Tc}$ -endothelin derivative, regardless of the diet after intervention (Fig. 2B).

Quantitative autoradiography of the excised aorta revealed good correlation of  $^{99m}\text{Tc}$ -endothelin derivative accumulation and the atherosclerotic lesions stained with sudan-III (Fig. 3). Accumulation of the  $^{99m}\text{Tc}$ -endothelin derivative in the untreated vessels was not significantly different whether with or without cholesterol feeding and amounted to  $170 \pm 5$  cpm/mm<sup>2</sup> and  $156 \pm 16$  cpm/mm<sup>2</sup>, respectively. In the induced lesions of the infrarenal aorta, accumulation of the  $^{99m}\text{Tc}$ -endothelin derivative was only slightly higher ( $1160 \pm 280$  cpm/mm<sup>2</sup>) with cholesterol feeding compared with animals without cholesterol feeding ( $983 \pm 342$  cpm/mm<sup>2</sup>) after balloon denudation. The ratio of accumulation between the induced lesions and untreated vessel wall was  $6.8 \pm 1.4$  in the cholesterol-fed animals and  $6.3 \pm 1.8$  in the animals without cholesterol feeding.

Histological and immunohistochemical analyses of the infrarenal aorta revealed that balloon denudation without cholesterol diet led to formation of a neointima ( $0.76 \pm 0.27$  mm<sup>2</sup>) with a high number of smooth muscle cells ( $1018 \pm 233$  cells per cross-section) but only a few macrophages ( $177 \pm 213$ ). Cholesterol diet during plaque development led to an increase in neointimal area ( $2.6 \pm 1.7$  mm<sup>2</sup>) and high levels of both smooth muscle cells ( $1222 \pm 171$ ) and macrophages ( $1270 \pm 1027$ ). The number of smooth muscle cells in the media was not affected by diet, because it was not significantly different in animals with ( $1943 \pm 230$ ,  $n = 4$ ) and without ( $2148 \pm 397$ ,  $n = 4$ ) cholesterol feeding after endothelial denudation. Accumulation of  $^{99m}\text{Tc}$ -endothelin derivative correlated well with

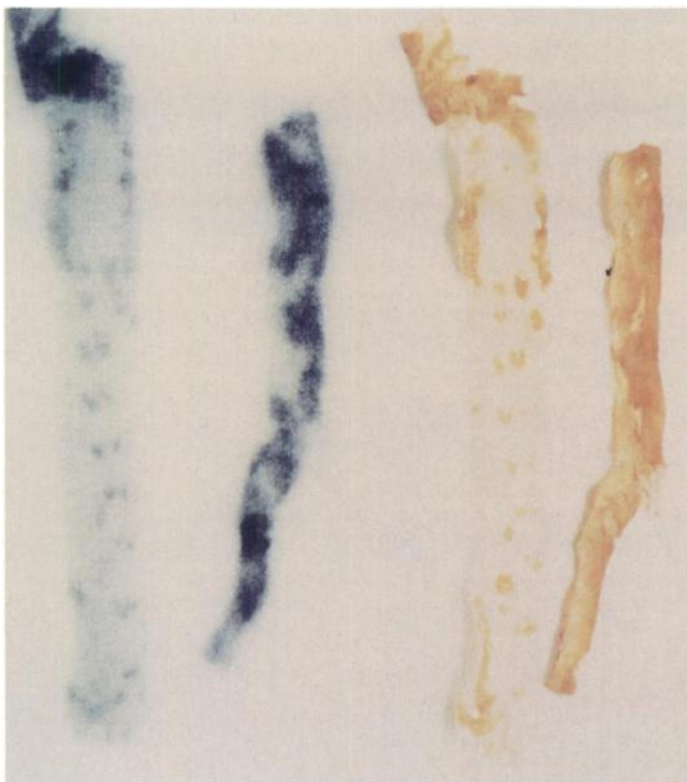


**FIGURE 3.** Quantitative autoradiography (left) and sudan-III staining (right) of an aorta from balloon-denuded rabbit fed a 0.5% cholesterol diet. Note that aorta is depicted in two portions. On the left are aortic arch, thoracic aorta and part of abdominal aorta. On the right are infrarenal aorta, bifurcation and parts of both iliac arteries. Ratio of accumulation between atherosclerotic lesions and normal vessel wall was  $6.8 \pm 1.4$  ( $n = 4$ ) in cholesterol-fed animals and  $6.3 \pm 1.8$  ( $n = 4$ ) in animals without cholesterol feeding.

the number of smooth muscle cells in the neointima (Fig. 4, correlation coefficient = 0.924) by interindividual comparison. No correlation of either the number of macrophages and medial smooth muscle cells, the area of the neointima or the maximum thickness of the neointima was observed.

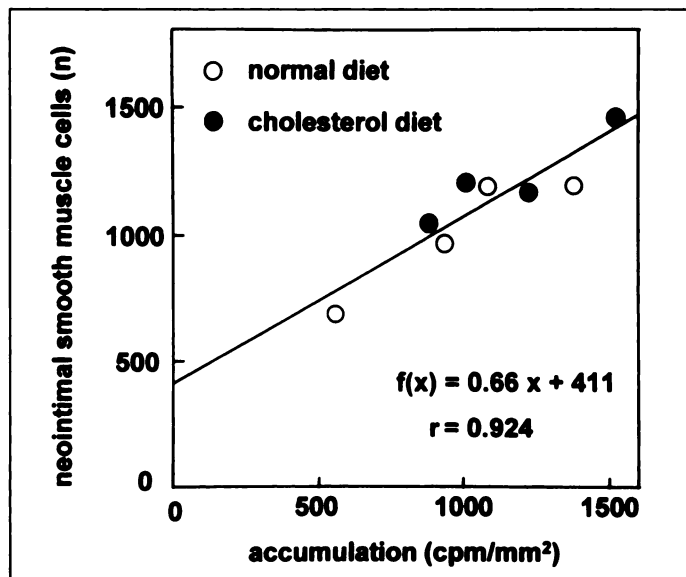


**FIGURE 4.** Correlation of  $^{99m}\text{Tc}$ -endothelin derivative accumulation with number of vascular smooth muscle cells in neointima. Accumulation of  $^{99m}\text{Tc}$ -endothelin derivative correlates with number of smooth muscle cells in neointima (correlation coefficient = 0.924) by interindividual comparison. No correlation of number of macrophages, neointimal area or maximum neointimal thickness was observed.

## DISCUSSION

A noninvasive, disease-specific, whole-body screening technique for the localization and quantitative assessment of early stages of atherogenesis is of great importance. Atherosclerosis is characterized partly by the proliferation and migration of vascular smooth muscle cells. Besides being the most potent vasoconstrictors in mammals, endothelins influence cell proliferation. Therefore, endothelins have been implicated in cardiovascular disorders ranging from hypertension to ischemia, stroke, and atherosclerosis (8,9). The plasma endothelin 1 level after percutaneous transluminal coronary angioplasty and in patients suffering from atherosclerosis is elevated, and endothelin 1 immunoreactivity is increased in active human plaque tissue (10–12). Endothelin 1 has been reported to be a potent mitogen in fibroblasts and rat aortic smooth muscle cells (13,14). Wang et al. (15) found an increased receptor expression of endothelin-converting enzyme-1, endothelin-1 and endothelin-3 after balloon angioplasty in rat carotid arteries. In fact, intra-arterial administration of endothelin 1 augmented the degree of neointimal formation dose dependently in the rat balloon injury model (16). In human atherosclerotic lesions, messenger ribonucleic acid of endothelin receptors is expressed (17). In fibrofatty plaques of cholesterol-fed hamsters, endothelin receptor messenger ribonucleic acid was detected in aortic endothelial cells, neointimal smooth muscle, macrophage-foam cells, and, to a lesser extent, medial smooth muscle cells (18). In human atherectomy specimens, the strongest endothelin-1-like immunoreactivity was found in foamy macrophages and alpha-actin-positive myofibroblasts in cell-rich areas of plaques (19). Blockade of endothelin receptors induced regression of atherosclerosis in cholesterol-fed hamsters and led to a decrease in neointimal plaque size in the rat denudation model (16,18). Binding of  $^{125}\text{I}$ -labeled endothelins to atherosclerotic human vessels in vitro was increased compared with that to control vessels (20).

We report evidence of scintigraphic visualization of experimentally induced atherosclerosis using a  $^{99m}\text{Tc}$ -endothelin derivative in vivo. Accumulation of this  $^{99m}\text{Tc}$ -endothelin derivative correlated with the number of smooth muscle cells but not with the amount of macrophages, the area or the maximum thickness of the neointima. Therefore, we assume that accumulation of the  $^{99m}\text{Tc}$ -endothelin derivative in neointimal lesions is due to binding to proliferated neointimal smooth muscle cells.

In general, a correlation of the accumulation of the endothelin derivative and the atherosclerotic lesions could be demonstrated (Fig. 3). However, especially in the infrarenal and iliac lesions induced by balloon denudation, there are some areas with more sudan staining than radioactivity and vice versa. This could be due to the fact that sudan-III only stains the lipid components of the lesions, which do not necessarily correlate with the regions of intensive smooth muscle cell proliferation.

The proliferation of smooth muscle cells is only one characteristic parameter of atherogenesis. Other parameters include infiltration of lipids, cellular invasion of macrophages and lymphocytes, calcification and thrombus formation. Therefore, the value of assessing the amount of or the proliferation of neointimal smooth muscle cells for the characterization of atherosclerotic lesions has still to be demonstrated. At least monitoring of restenosis, which is mainly due to proliferation of smooth muscle cells, should be feasible.

We are now investigating the mechanisms of accumulation of the endothelin derivative and its potential to differentiate between instable proliferative and stable atherosclerotic lesions.

## CONCLUSION

The investigated  $^{99m}\text{Tc}$ -labeled endothelin derivative allows screening of atherosclerosis in animals. The accumulation of the endothelin derivative in induced atherosclerotic lesions correlates with the neointimal amount of smooth muscle cells. Therefore, the endothelin derivative may be useful in gaining information on the cellular composition or the proliferative status of atherosclerotic lesions.

## ACKNOWLEDGMENTS

The authors thank Eva Maria Bickel and Ingolf Weber for their excellent technical assistance. A preliminary account of this work was published in abstract form (5).

## REFERENCES

1. Ross R. The pathogenesis of atherosclerosis: a perspective for the 1990s. *Nature* 1993;362:801-809.
2. Hanke H, Strohschneider T, Oberhoff M, Betz E, Karsch KR. Time course of smooth muscle cell proliferation in the intima and media of arteries following experimental angioplasty. *Circ Res* 1990;67:651-659.
3. Sakurai T, Yanagisawa M, Masaki T. Molecular characterization of endothelin receptors. *Trends Pharmacol Sci* 1992;13:103-108.
4. Takuwa Y, Kasuya Y, Takuwa N, et al. Endothelin receptor is coupled to phospholipase C via a pertussis toxin-insensitive guanine nucleotide-binding regulatory protein in vascular smooth muscle cells. *J Clin Invest* 1990;85:653-658.
5. Dinkelborg LM, Duda S, Hanke H, Tepe G, Hilger CS, Semmler W. Characterization of a technetium-99m-endothelin derivative for imaging of atherosclerosis in a rabbit balloon denudation model. *J Nucl Med* 1997;38(suppl):173P.
6. Doherty AM, Cody WL, DePue PL, et al. Structure-activity relationships of C-terminal endothelin hexapeptide antagonists. *J Med Chem* 1993;36:2585-2594.
7. Johannsen B, Jankowsky R, Noll B, et al. Technetium coordination ability of cysteine-containing peptides: x-ray absorption spectroscopy of a  $^{99m}\text{Tc}$ -labelled endothelin derivative. *Appl Radiat Isot* 1997;48:1045-1050.
8. Rubanyi GM, Polokoff MA. Endothelins: molecular biology, biochemistry, pharmacology, physiology, and pathophysiology. *Pharmacol Rev* 1994;46:325-415.
9. Goto K, Warner TD. Molecular pharmacology. Endothelin versatility. *Nature* 1995;375:539-540.
10. Lerman A, Edwards BS, Hallett JW, Heublein DM, Sandberg SM, Burnett JC Jr. Circulating and tissue endothelin immunoreactivity in advanced atherosclerosis. *N Engl J Med* 1991;325:997-1001.
11. Tahara A, Kohno M, Yanagi S, et al. Circulating immunoreactive endothelin in patients undergoing percutaneous transluminal coronary angioplasty. *Metabolism* 1991;40:1235-1237.
12. Zeiher AM, Goebel H, Schachinger V, Ihling C. Tissue endothelin-1 immunoreactivity in the active coronary atherosclerotic plaque. A clue to the mechanism of increased vasoreactivity of the culprit lesion in unstable angina. *Circulation* 1995;91:941-947.
13. Hirata Y, Takagi Y, Fukuda Y, Marumo F. Endothelin is a potent mitogen for rat vascular smooth muscle cells. *Atherosclerosis* 1989;78:225-228.
14. Bobik A, Grooms A, Millar JA, Mitchell A, Grinpukel S. Growth factor activity of endothelin on vascular smooth muscle. *Am J Physiol* 1990;258:C408-C415.
15. Wang X, Douglas SA, Loudon C, Vickery Clark LM, Feuerstein GZ, Ohlstein EH. Expression of endothelin-1, endothelin-3, endothelin-converting enzyme-1, and endothelin-A and endothelin-B receptor mRNA after angioplasty-induced neointimal formation in the rat. *Circ Res* 1996;78:322-328.
16. Douglas SA, Loudon C, Vickery Clark LM, et al. A role for endogenous endothelin-1 in neointimal formation after rat carotid artery balloon angioplasty. Protective effects of the novel nonpeptide endothelin receptor antagonist SB 209670. *Circ Res* 1994;75:190-197.
17. Winkles JA, Alberts GF, Brogi E, Libby P. Endothelin-1 and endothelin receptor mRNA expression in normal and atherosclerotic human arteries. *Biochem Biophys Res Commun* 1993;191:1081-1088.
18. Kowala MC, Rose PM, Stein PD, et al. Selective blockade of the endothelin subtype A receptor decreases early atherosclerosis in hamsters fed cholesterol. *Am J Pathol* 1995;146:819-826.
19. Ihling C, Gobel HR, Lippoldt A, et al. Endothelin-1-like immunoreactivity in human atherosclerotic coronary tissue: a detailed analysis of the cellular distribution of endothelin-1. *J Pathol* 1996;179:303-308.
20. Dashwood MR, Sykes RM, Muddle JR, et al. Autoradiographic localization of [ $^{125}\text{I}$ ]endothelin binding sites in human blood vessels and coronary tissue: functional correlates. *J Cardiovasc Pharmacol* 1991;17(suppl 7):S458-S462.

---

# Renal Depth Estimates to Improve the Accuracy of Glomerular Filtration Rate

Adam P. Steinmetz, S. Tzila Zwas, Sorina Macadziob, Galina Rotemberg and Ygal Shrem

Department of Nuclear Medicine, Chaim Sheba Medical Center, Tel Hashomer; Sackler School of Medicine, Tel-Aviv University, Tel-Aviv; and Elscint Ltd., Haifa, Israel

---

This study was performed to validate a computer implementation of the Gates' method for radionuclide glomerular filtration rate (RGFR) calculation. The accuracy of the original method was improved by replacing the Tonnesen formula that estimated renal depth with direct measurement from lateral views to calculate tissue attenuation correction. **Methods:** Both the creatinine clearance test (CCT) and dynamic  $^{99m}\text{Tc}$ -diethylenetriamine pentaacetic acid (DTPA) renal scintigraphy (DRS) were performed on 38 patients on the same day. RGFR was quantified from the attenuation corrected absolute DTPA uptake of the kidneys on DRS from 120-180 sec after injection. Attenuation correction was estimated using the lateral views of the kidneys taking in account the distance from the computed geometric center of the kidneys to the posterior body surface along a line vertical to the collimator surface. CCT and glomerular filtration rate estimates from DRS were compared by linear regression. **Results:** RGFR estimates agreed well with CCT, yielding a correlation coefficient of 0.92 in 38 patients and 0.90 in a subgroup of 11 patients suffering from chronic renal failure. **Conclusion:** Present modifications improve RGFR accuracy to the

precision range of blood sample based methods. This modified method requires little additional work and no extra cost in patients undergoing DRS. RGFR calculation may be advantageous in cases when 24-hr urine collection for CCT cannot be obtained, and it should improve the accuracy of the captopril test.

**Key Words:** glomerular filtration rate; kidney radionuclide imaging; technetium-99m-diethylenetriamine pentaacetic acid

*J Nucl Med* 1998; 39:1822-1825

---

**B**y the request of a nuclear medicine hardware manufacturer (Elscint, Haifa, Israel) validation of a computer program calculating glomerular filtration rate (GFR) based on the Gates' method (1-3) was undertaken. The precision of the original method was significantly improved by replacing the Tonnesen formula by direct measurement of the kidney depth from lateral views, thus improving the accuracy of tissue attenuation correction of the renal uptake.

## MATERIALS AND METHODS

Fifty patients were included in the study group (20 women, 30 men; age range 7-84 yr, including 3 children; mean age 44 yr).

---

Received Nov. 21, 1996; revision accepted Jan. 12, 1998.

For correspondence or reprints contact: S. Tzila Zwas, MD, Department of Nuclear Medicine, Chaim Sheba Medical Center, Tel-Hashomer, Ramat-Gan 52621, Israel.